Structural Studies on the Synchronization of Catalytic Centers in Glutamate Synthase*

Robert H. H. van den Heuvel‡§, Davide Ferrari¶, Roberto T. Bossi‡, Sergio Ravasio‖, Bruno Curti‖, Maria A. Vanoni, Francisco J. Florencio‡‡, and Andrea Mattevi‡§§**

*From the ‡Department of Genetics and Microbiology, University of Pavia, via Abbiategrasso 207, 27100 Pavia, the ¶Department of Biochemistry and Molecular Biology, University of Parma, Parco Area delle Scienze 23/A, 43100 Parma, the ‖Department of General Physiology and Biochemistry, University of Milan, via Celoria 26, 20133 Milan, the **Department of Chemical, Physical and Mathematical Sciences, University of Insubria, via Valleggio 11, 22100 Como, Italy, and ‡‡Institute of Plant Biochemistry and Photosynthesis, University of Sevilla-CSIC, Avenida Américo Vespucio s/n, 41092 Sevilla, Spain*

The complex iron-sulfur flavoprotein glutamate synthase (GltS) plays a prominent role in ammonia assimilation in bacteria, yeasts, and plants. GltS catalyzes the formation of two molecules of L-glutamate from 2-oxoglutarate and L-glutamine via intramolecular channeling of ammonia. GltS has the impressive ability of synchronizing its distinct catalytic centers to avoid wasteful consumption of L-glutamine. We have determined the crystal structure of the ferredoxin-dependent GltS in several ligation and redox states. The structures reveal the crucial elements in the synchronization between the glutaminase site and the 2-iminoglutarate reduction site. The structural data combined with the catalytic properties of GltS indicate that binding of ferredoxin and 2-oxoglutarate to the FMN-binding domain of GltS induce a conformational change in the loop connecting the two catalytic centers. The rearrangement induces a shift in the catalytic elements of the amidotransferase domain, such that it becomes activated. This machinery, over a distance of more than 30 Å, controls the ability of the enzyme to bind and hydrolyze the ammonia-donating substrate L-glutamine.
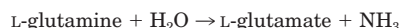
Substrate channeling is the process of direct transfer of a reaction intermediate between enzyme-active sites that catalyze sequential reactions in a biosynthetic pathway (1). The active sites can either be located on separate subunits in a multienzyme complex or in separate domains in multifunctional enzymes. Direct transfer between the enzyme-active sites prevents loss of the intermediate into solution, limits the entrance of the intermediate into competing processes, protects labile intermediates from degradation in solution, and increases the success rate of the catalytic cycle by lowering the probability of uncoupled consecutive reactions (2, 3).
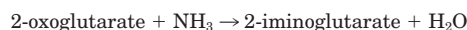
Glutamine amidotransferases play a central role in cellular metabolism as they provide the main route for the incorporation of nitrogen into various biomolecules. These well studied enzymes catalyze two reactions at separate catalytic centers. L-Glutamine is hydrolyzed in the glutaminase site yielding ammonia, which is, in the subsequent synthase reaction, added to an acceptor substrate that varies among the different glutamine amidotransferases. Structural and functional studies have revealed that glutamine amidotransferases function through the channeling of ammonia from the glutaminase site to the synthase site (3, 4). In phosphoribosylpyrophosphate amidotransferase channel formation appeared to be dependent on the substrate binding to the synthase site (5), whereas in, for example, asparagine synthetase B, imidazoleglycerol-phosphate synthase, and glucosamine-6-phosphate synthase permanent channels were observed (6–8).

Glutamate synthase (GltS)[1] is a key enzyme in the early stages of the assimilation of ammonia in bacteria, yeasts, and plants. The enzyme is a complex iron-sulfur flavoprotein catalyzing the reductive transfer of the amido nitrogen from L-glutamine to 2-oxoglutarate to form two molecules of L-glutamate (Scheme 1). In bacteria, L-glutamate is involved in osmoregulation (9), is the precursor for other amino acids, and can be the precursor for heme biosynthesis (10). In plants, GltS is especially essential in the reassimilation of ammonia released by photorespiration.

Amidotransferase domain

$$\text{L-glutamine} + \text{H}_2\text{O} \rightarrow \text{L-glutamate} + \text{NH}_3$$

FMN-binding domain

$$\text{2-oxoglutarate} + \text{NH}_3 \rightarrow \text{2-iminoglutarate} + \text{H}_2\text{O}$$

$$2e^- + \text{FMN}_{ox} \rightarrow \text{FMN}_{red}$$

$$\text{2-iminoglutarate} + \text{FMN}_{red} \rightarrow \text{L-glutamate} + \text{FMN}_{ox}$$

SCHEME 1

On the basis of the amino acid sequence and the nature of the electron donor, three different classes of GltS can de defined as follows: 1) ferredoxin-dependent GltS (Fd-GltS), 2) NADPH-dependent GltS (NADPH-GltS), and 3) NADH-dependent GltS

[1] The abbreviations used are: GltS, glutamate synthase; Fd, ferredoxin; Fd loop, residues 907–933; loop 4, residues 968–1013; Ntn-amidotransferase, N-terminal nucleophile amidotransferase; r.m.s.d., root mean square deviation; Pipes, 1,4-piperazinediethanesulfonic acid.

TABLE I
X-ray data collection and refinement statistics

	Native Fd-GltS[a]	Fd-GltS, 2-oxoglutarate[b]	Reduced Fd-GltS
Data collection			
Resolution range (Å)	62–2.8	62–2.7	55–3.0
Cell dimensions (Å)	$a = 166.08$	$a = 166.52$	$a = 167.00$
	$b = 166.08$	$b = 166.52$	$b = 167.00$
	$c = 219.58$	$c = 219.87$	$c = 221.03$
Observed	1,595,358	947,721	487,880
Unique reflections	76,995	83,666	62,124
Completeness (%)[c]	99.4 (96.6)	98.1 (92.7)	97.1 (98.4)
R_{merge}[c,d]	12.0 (45.5)	8.8 (28.9)	9.3 (29.6)
Intensities (I/σ)[c]	3.8 (1.7)	4.5 (2.3)	5.7 (1.8)
Refinement			
R_{factor}[e]	23.6	23.4	21.7
R_{free}[c]	28.7	29.3	26.9
No. atoms	11,395	11,408	11,349
Ligand	8 (two acetates)	10 (2-oxoglutarate)	0
Water molecules	38	49	0
R.m.s. bond length	0.021	0.020	0.018
R.m.s. bond angle	2.23	2.20	2.05
Average B value	35.2	41.2	35.9

[a] No ligands were included.

[b] Structures were obtained from both Fd-GltS co-crystallized with L-methionine sulfone/2-oxoglutarate and 6-diazo-5-oxo-L-norleucine/2-oxo-glutarate. Throughout this work, we only refer to Fd-GltS co-crystallized with L-methionine sulfone/2-oxoglutarate.

[c] Numbers in parentheses correspond to data in the outermost resolution shell.

[d] $R_{merge} = \Sigma |I_j - <I>|/\Sigma <I_j>$, where I_j is the intensity of an observation of reflection j and $<I_j>$ is the average intensity for reflection j.

[e] $R_{factor} = \Sigma |F_{obs}| - |F_{calc}||/\Sigma F_{obs}$; R_{free} for 2.5% subset of reflections.

(properties of the three classes have been reviewed extensively (11)). Fd-GltS functions through the non-covalent binding of ferredoxin (Fd), which delivers reducing equivalents to the FMN cofactor via a 3Fe-4S cluster (12). The NADPH-GltS is catalytically active as a $\alpha\beta$-heterodimer in which the β-subunit serves as the electron donor for L-glutamate formation within the α-subunit (11, 13). Fd-GltS and the α-subunit of the NADPH-GltS (α-GltS) share considerable homology throughout their amino acid sequences. Despite this homology, Fd-GltS and α-GltS display a remarkable difference in the synchronization between the catalytic centers. α-GltS has significant glutaminase activity, indicative of weak coupling between the catalytic centers (14). In contrast, Fd-GltS is tightly coupled and lacks any glutaminase activity.[2]

Recently, the three-dimensional structure of *Azospirillum brasilense* α-GltS has been determined (16). This crystal structure provided us with a new example of ammonia channeling and interdomain communication by N-terminal nucleophile (Ntn) amidotransferases. In this paper, we present the crystal structure of the Fd-GltS from the cyanobacterium *Synechocystis* sp. PCC 6803. This enzyme of 165 kDa contains one FMN cofactor and one 3Fe-4S cluster as prosthetic groups (12). The three-dimensional structure was solved in different ligation and redox states, giving us new insights in the structural basis for synchronization and channeling between catalytic centers.

EXPERIMENTAL PROCEDURES

Protein Expression, Purification, and Crystallization—The *gls*F gene from *Synechocystis* sp. PCC 6803 was cloned, overexpressed in the glutamate auxotrophic *Escherichia coli* strain CLR207 *RecA,* and purified as described previously (12).

Crystals of Fd-GltS were obtained at 4 °C by using the hanging-drop vapor diffusion method. The enzyme solution contained 16 mg/ml in 25 mM Pipes/KOH, pH 7.0, 1 mM EDTA, and 10% glycerol. The reservoir solution contained 24–30% (w/v) polyethylene glycol 4000, 100 mM Tris-hydrochloride, pH 8.5, and 200 mM sodium acetate. Liganded enzyme was prepared by the addition of 4 mM L-methionine sulfone or 4 mM 6-diazo-5-oxo-L-norleucine, 2 mM 2-oxoglutarate, and 5 mM dithiothreitol prior to crystallization. Reduction of the Fd-GltS crystals was obtained by soaking the enzyme crystal with 2 mM L-glutamate at room

temperature for 90 min. The redox state of the crystal upon the addition of L-glutamate was followed by single crystal microspectrophotometry. The crystal in its soaking solution with L-glutamate was placed in a quartz cell and reduction of the FMN and 3Fe-4S cluster was measured under aerobic conditions as a function of time (Zeiss MPM800) (17).

Data Collection and Processing—Before data collection, the crystals were cryoprotected by the reservoir solution plus 25% (v/v) 2-methyl-2,4-pentanediol and flash-frozen in a nitrogen stream at 100 K. All diffraction data were recorded on beamline ID14-EH1 at the European Synchrotron Radiation Facility (Grenoble, France) using a MarCCD detector. Data were integrated by MOSFLM (18) and further processed with programs from the CCP4 package (19). Fd-GltS crystals belong to space group P4$_3$2$_1$2 with unit cell axes $a = b = 166.08$ Å and $c = 219.58$ Å. Data processing statistics are reported in Table I.

Structure Determination—The structure of Fd-GltS from *Synechocystis* sp. PCC 6803 was solved by molecular replacement with the program MOLREP (20) using the structure of α-GltS from *A. brasilense* as a search model (16). The initial map was improved by solvent flattening and histogram matching (21). The initial model, built with the program O (22), was subjected to maximum likelihood refinement with REFMAC (20). Progress of the refinement was monitored by the free R factor (24). The positions of ordered water molecules were determined using the program ARP (25). Refinement statistics are shown in Table I. The final model includes one polypeptide chain with a total of 1472 residues (residues 1–422, 439–534, 540–812, and 824–1507), one 3Fe-4S cluster, one FMN, two acetate ions, and 38 water molecules. 81.3% of the amino acids are in the core region of the Ramachandran plot (26).

The refined atomic coordinates of native Fd-GltS were used as the starting model for the determination of the structures of Fd-GltS co-crystallized with L-methionine sulfone/2-oxoglutarate and 6-diazo-5-oxo-L-norleucine/2-oxoglutarate and of Fd-GltS reduced by L-glutamate. After rigid body refinement, the structures of the complexes were refined with REFMAC (23), and the same set of reflections as those for the native structure were excluded to calculate the free R factor. Because L-methionine sulfone and 6-diazo-5-oxo-L-norleucine did not bind to the L-glutamine-binding site, two identical structures with 2-oxoglutarate bound were refined. In this paper, we refer to the 2-oxoglutarate complexed Fd-GltS as the enzyme co-crystallized with L-methionine sulfone/2-oxoglutarate.

VOIDOO (27), PROCHECK (26), CLUSTAL (28), and programs from the CCP4 package (19) were used for structure analysis. Figures were produced by MOLSCRIPT (29), BOBSCRIPT (30), and Raster3D (31).

RESULTS AND DISCUSSION

Overall Structure—Crystals of *Synechocystis* sp. Fd-GltS were grown in the native state (no ligands), in the presence of 2-oxoglutarate and L-methionine sulfone and of 2-oxoglutarate

[2] Ravasio, S., Dossena, L., Martin-Figueroa, E., Florencio, F. J., Mattevi, A., Morandi, P., Curti, B., and Vanoni, M. A. (2002) *Biochemistry*, in press.
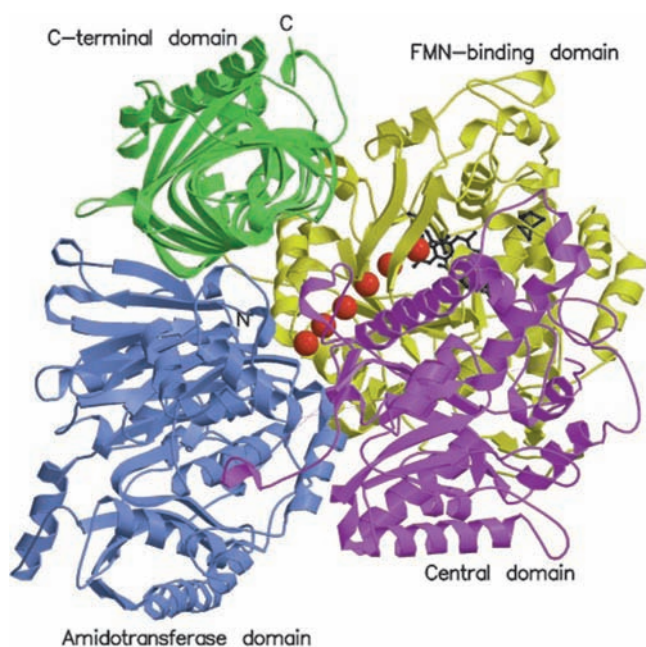
FIG. 1. **The overall structure of Fd-GltS with the N-terminal amidotransferase domain depicted in *cornflower blue*, the FMN-binding domain in *yellow*, the central domain in *magenta*, and the C-terminal domain in *green*.** The FMN cofactor and the 3Fe-4S cluster are shown in *black ball-and-stick*, and the ammonia channel is outlined by *red spheres*. *Dashed lines* connect the borders of disordered loops.

FIG. 2. **The glutaminase site of GltS.** *A*, the stereo view drawing was obtained by superimposing α-GltS onto Fd-GltS. Fd-GltS is depicted in *dark gray*, and α-GltS including the bound L-methionine sulfone (*L-MetS*) substrate analog is depicted in *light gray*. Atoms within hydrogen bond distance are connected by *dashed lines.* Note that loop 4 (residues 968–1013) and Glu-1013 belong to the FMN-binding domain (numbering according to Fd-GltS). *B*, stereo view drawing of the experimental $2F_o - F_c$ electron density map at 2.7 Å using the final model, contoured at 1.0 σ. The orientation in both figures is identical to that of Fig. 1.

and 6-diazo-5-oxo-L-norleucine. Moreover, the structure of Fd-GltS with FMN in the reduced state was obtained by crystal soaking with the reaction product L-glutamate, which is able to reduce the flavin cofactor and the 3Fe-4S cluster.[2] The overall structure as well as the geometry of the catalytic centers in all these complexes are virtually identical with root mean square deviations (r.m.s.d.) calculated from pairwise superpositions of less than 0.2 Å for equivalent Cα atoms. Unless stated otherwise, for the analysis of the model we shall refer to the structure resulting from the co-crystallization with 2-oxoglutarate/L-methionine sulfone solved at a resolution of 2.7 Å (Table I).

Fd-GltS is a 1523-residue enzyme, which is composed of four structurally and functionally distinct domains (Fig. 1). The overall topology of the N-terminal amidotransferase domain (residues 1–422) is characterized by a four layer α/β/β/α architecture and is similar to other Ntn-amidotransferases (15). The amidotransferase domain from Fd-GltS contains the typical catalytic center of Ntn-amidotransferases, and the N-terminal Cys-1 catalyzes the hydrolysis of L-glutamine generating ammonia and the first molecule of L-glutamate (Scheme 1).

The FMN-binding domain (residues 787–1239) of Fd-GltS is characterized by a classic $(\beta/\alpha)_8$ barrel. In the FMN-binding domain the 2-iminoglutarate intermediate, formed upon the addition of ammonia onto 2-oxoglutarate, is reduced by the FMN cofactor producing the second molecule of L-glutamate (Scheme 1). This domain also contains the enzyme 3Fe-4S cluster, which participates in the transfer of electrons from the Fd molecule to the FMN cofactor.

The central domain (residues 423–786) is connecting the amidotransferase domain with the FMN-binding domain and has an α/β overall topology. The C-terminal domain (residues 1240–1507) has a right-handed β-helix topology composing seven β-helical turns. This domain does not have a direct function in glutamate synthase activity but rather a structural function through extensive interactions with the amidotransferase and FMN-binding domains (16).

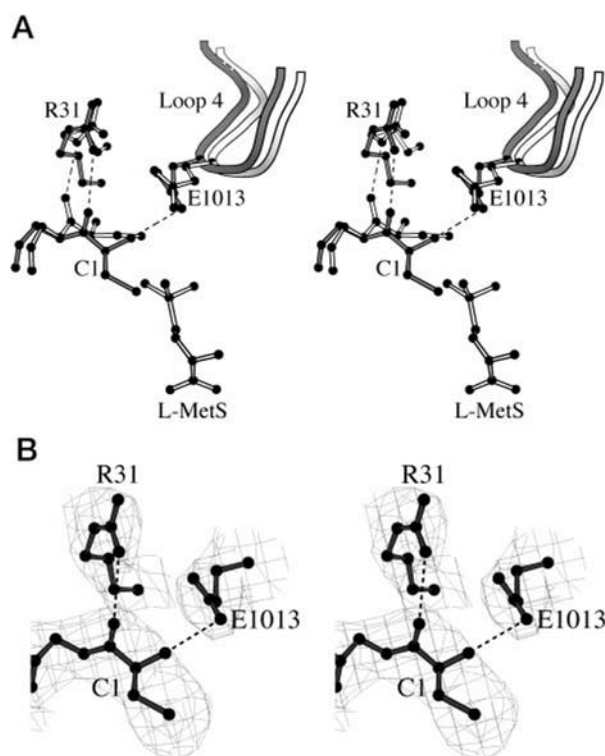This four-domain architecture of Fd-GltS closely resembles

that of *A. brasilense* α-GltS (16). Superposition of the two structures results in a r.m.s.d. of 1.7 Å for 1403 topologically equivalent Cα atoms (45% sequence identity). However, the comparison between the enzymes reveals some crucial differences in their functional sites that lead to a better understanding of the mechanism of synchronization between the catalytic centers in GltSs.

Amidotransferase Domain—Superposition of the amidotransferase domains from Fd-GltS and α-GltS reveals a large difference in the L-glutamine-binding pocket. Here Cys-1 of Fd-GltS is shifted by 5 Å as compared with α-GltS (Fig. 2*A*). The electron density of the L-glutamine-binding pocket in Fd-GltS is well defined and allows the unambiguous positioning of Cys-1 (Fig. 2*B*). The N-terminal Cys residue is held in position by forming hydrogen bonds to OE2 of Glu-1013 from the FMN-binding domain and NH1 of Arg-31, which is a strictly conserved residue in Ntn-amidotransferases (15). Conversely, the N-terminal Cys residue in α-GltS cannot form a hydrogen bond with Glu-978 (homologous to Glu-1013 of Fd-GltS; Fig. 2*A*). The interaction between Cys-1 and Arg-31 in Fd-GltS can only occur due to the shift of the backbone of loop 31–39 and of the preceding α-helix (residues 15–30). The Cα atom of residue Arg-31 has moved 3.2 Å away with respect to the corresponding Arg-31 of α-GltS. The conformational changes in the L-glutamine-binding site create a solvent-accessible environment for Cys-1, whereas Cys-1 in α-GltS is shielded from the solvent (16).

The shift in the position of Cys-1 observed in Fd-GltS dramatically alters the geometry of the L-glutamine-binding pocket with respect to that found in α-GltS (Fig. 2*A*) (16).
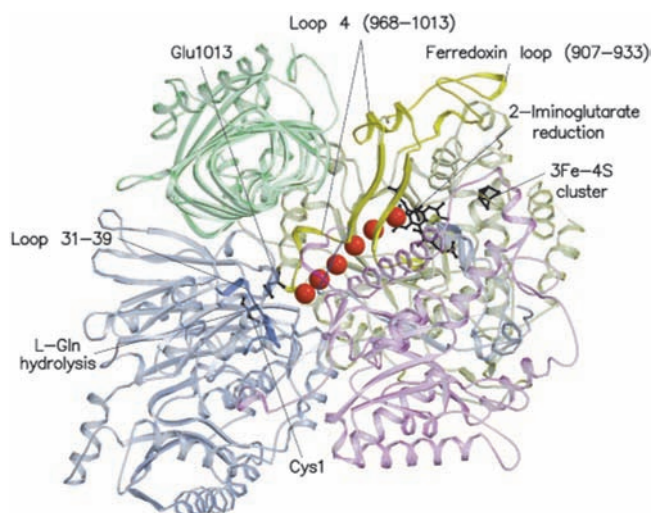
FIG. 3. **Interdomain communication in Fd-GltS.** The transparent coloring of the Fd-GltS monomer is identical to the coloring of the Fig. 1 as is the orientation. Highlighted are the proposed elements involved in interdomain channeling and synchronization; Fd loop (residues 907–933), loop 4 (residues 968–1013), and loop 31–39. The FMN cofactor, 3Fe-4S cluster, and residues Cys-1 and Glu-1013 are shown as *black ball-and-stick*. The ammonia channel is outlined by *red spheres.*

Indeed, no binding of substrate analogs in the L-glutamate-binding pocket was observed for any of the structures obtained by co-crystallization with L-methionine sulfone or 6-diazo-5-oxo-L-norleucine. Conversely, co-crystallization of α-GltS with L-methionine sulfone resulted in binding of the substrate analog in the enzyme-active site (16). This is in keeping with the functional data, which show that the glutaminase site is active in α-GltS (14) and inactive in Fd-GltS.[2] Superposition of Fd-GltS and α-GltS with bound L-methionine sulfone readily demonstrates that the glutaminase site of Fd-GltS is in an inactive conformation in which the analog binding is made sterically impossible by the movement of Cys-1 (Fig. 2*A*). Thus, the enzyme cannot consume any L-glutamine in this conformation.

FMN-binding Domain—The FMN-binding domains of Fd-GltS and α-GltS are highly similar. However, in Fd-GltS two long insertions occur at positions 813–822 and 907–933. The first insertion is unlikely to be of any structural or catalytic importance as it is not conserved among the GHS sequences. In contrast, the second insertion forms a loop, whose conformation is well defined by the electron density. This loop is located in the neighborhood of the 3Fe-4S cluster, at a distance of about 14 Å (Fig. 3), and is conserved among all Fd-dependent GltSs, but not in the NAD(P)H-dependent enzymes (11). Together, these observations suggest that this second insertion is involved in the binding of Fd (hereafter referred to as "Fd loop"). Binding at this position would allow electron transfer from Fd to the 3Fe-4S cluster, which would then donate the electrons to the isoalloxazine ring of the FMN cofactor.

The FMN and the 3Fe-4S cluster are located at 8 Å distance from each other in an identical position as observed in the structure of α-GltS (Fig. 4*A*) (16). The strictly conserved Met-475 bridges the two redox centers and is likely to be involved in electron transfer between the FMN and the cluster. The 2-oxoglutarate substrate is well defined in the electron density map resulting from the analysis of the protein co-crystallized with this substrate. 2-Oxoglutarate binds in front of the flavin and is maintained in the proper orientation for ammonia addition and subsequent reduction by interaction with Lys-972, Arg-992, and Thr-1065. This binding geometry is similar to that found in α-GltS. To investigate whether the binding of 2-oxoglutarate induces a conformational change in the catalytic site of the
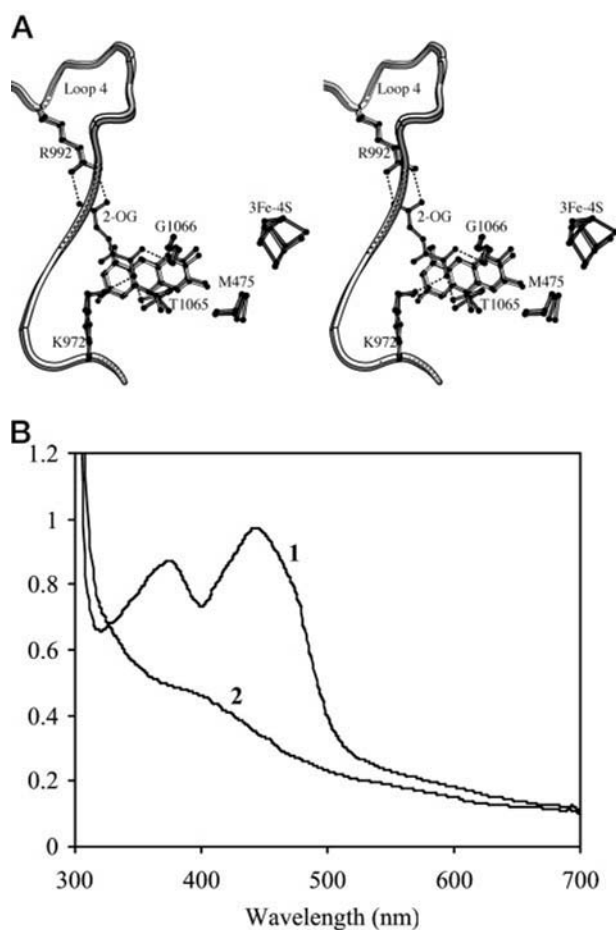
FIG. 4. **The 2-iminoglutarate reduction site upon L-glutamate reduction.** *A*, the stereo view drawing was obtained by superimposing the L-glutamate-reduced Fd-GltS onto the 2-oxoglutarate-bound Fd-GltS. The orientation is identical to Fd-GltS in Fig. 1. 2-Oxoglutarate-bound Fd-GltS is depicted in *dark gray*, and L-glutamate reduced Fd-GltS is depicted in *light gray*. Atoms within hydrogen bond distance are connected by *dashed lines*. *B*, polarized absorption spectrum of Fd-GltS crystal upon soaking with L-glutamate. Crystalline Fd-GltS in 30% (w/v) polyethylene glycol 4000, 100 mM Tris-hydrochloride, pH 8.5, and 200 mM sodium acetate was incubated by 2 mM L-glutamate under aerobic conditions. *Trace 1*, oxidized enzyme; *trace 2*, reduced enzyme.

FMN-binding domain, we also crystallized Fd-GltS in the absence of 2-oxoglutarate. The catalytic centers of the unliganded and liganded Fd-GltS appeared to be highly similar. However, this may be due to the presence of two acetate ions in the 2-oxoglutarate-binding site, which mimic the 2-oxoglutarate substrate.

Solution studies have shown that Fd-GltS reacts with its reaction product L-glutamate.[2] In this back reaction, L-glutamate first reduces the FMN cofactor after which it reduces the 3Fe-4S cluster (Scheme 1). To investigate the structural consequences of FMN and 3Fe-4S cluster reduction in GltS by L-glutamate, the crystals grown in the absence of 2-oxoglutarate were employed for a soaking experiment with L-glutamate. Indeed, this reaction product was able to react with the crystalline protein and to reduce the FMN cofactor and 3Fe-4S cluster as shown by crystal microspectrophotometry (Fig. 4*B*). However, FMN and 3Fe-4S reduction did not lead to any conformational changes in the flavin site or the catalytic centers of the amidotransferase and FMN-binding domains (Fig. 4*A*). These observations are fully consistent with kinetic studies[2] and indicate that Fd binding and not flavin reduction triggers the activation of the glutaminase site.

Interdomain Channeling and Synchronization—During cat-

alysis of Fd-GltS, ammonia produced by L-glutamine hydrolysis is channeled to the 2-oxoglutarate-binding site, in which 2-iminoglutarate is formed. The crystal structure of Fd-GltS with the inactive glutaminase site exhibits an intra-molecular channel of 24 Å (measured from the Cα atom of Ser-1011 to O2 of 2-oxoglutarate) from the 2-oxoglutarate-binding site to the main chain atoms of residues 503, 504, and 1011–1013 (Fig. 3). The backbone atoms of these five residues obstruct the channel and are located in the proximity of Cys-1.

The most striking functional feature of Fd-GltS is its ability to coordinate its catalytic centers such that it avoids wasteful consumption of L-glutamine when Fd and 2-oxoglutarate are not available. The kinetic characterization of Fd-GltS has shown that the binding of both Fd and 2-oxoglutarate is required to activate the glutaminase site.[2] The absence of any glutaminase activity in solution further highlights the tight coupling between the glutaminase site, 2-iminoglutarate reduction site, and Fd binding. The most important protein region for communication between the catalytic centers and Fd binding appears to be the strictly conserved polypeptide loop 4 in the FMN-binding domain (residues 968–1013) (Fig. 3). The N-terminal region of loop 4 is located in the proximity of the Fd loop with a direct contact between the OH of Tyr-987 (loop 4) and OD1 of Asp-907 (Fd loop). Further downstream, loop 4 wraps around the 2-oxoglutarate-binding site being hydrogen-bonded to 2-oxoglutarate through Arg-992 and Lys-972. At the C terminus, loop 4 lines the channel for the transfer of ammonia and with the C-terminal residue Glu-1013 it forms a hydrogen bond to the backbone nitrogen of Cys-1, thereby keeping the Cys-1 in the inactive conformation (Fig. 2).

We propose that binding of Fd and 2-oxoglutarate to the FMN-binding domain of Fd-GltS induces a conformational change in loop 4. This may be transduced to loop 4 C-terminal residues, which open the channel (residues 1011 and 1012) and move slightly the side chain of Glu-1013, thereby breaking the hydrogen bond with Cys-1 (Fig. 2). This may have the following effects in the glutaminase site. 1) Cys-1 shifts to a conformation in which it is able to bind the L-glutamine substrate. It is likely that Cys-1 takes up a conformation similar to that observed in the crystal structure of α-GltS in the catalytically active conformation bound to L-methionine sulfone (12) (Fig. 2). 2) The shift of Cys-1 induces a conformational change in loop 31–39, such that Arg-31 can make a hydrogen bond to Cys-1 and a salt bridge to Glu-1013. At this stage, L-glutamine can be hydrolyzed producing the first molecule of L-glutamate and ammonia to be channeled to the 2-oxoglutarate-binding site (Scheme 1). The crystal structure of Fd-GltS suggests the crucial elements in the synchronization between the catalytic centers: formation of the complex between Fd and Fd-GltS, 2-oxoglutarate binding to the FMN-binding domain, rear-

rangement of loop 4, and movement of Cys-1 and loop 31–39 in the amidotransferase domain. Such a sophisticated machinery allows the transduction of two activating signals (Fd and 2-oxoglutarate) across a distance of more than 30 Å, thereby controlling the ability of the enzyme to bind the ammonia-donating substrate L-glutamine.

REFERENCES

1. Srere, P. A. (1987) *Annu. Rev. Biochem.* **56,** 89–124
2. Ovadi, J. (1991) *J. Theor. Biol.* **152,** 135–141
3. Miles, E. W., Rhee, S., and Davies, D. R. (1999) *J. Biol. Chem.* **274,** 12193–12196
4. Raushel, F. M., Thoden, J. B., and Holden, H. M. (1999) *Biochemistry* **38,** 7891–7899
5. Krahn, J. M., Kim, J. H., Burns, M. R., Parry, R. J., Zalkin, H., and Smith, J. L. (1997) *Biochemistry* **36,** 11061–11068
6. Chaudhuri, B. N., Lange, S. C., Myers, R. S., Chittur, S. V., Davisson, V. J., and Smith, J. L. (2001) *Structure* **9,** 987–997
7. Larsen, T. M., Boehlein, S. K., Schuster, S. M., Richards, N. G., Thoden, J. B., Holden, H. M., and Rayment, I. (1999) *Biochemistry* **38,** 16146–16157
8. Teplyakov, A., Obmolova, G., Badet, B., and Badet-Denisot, M. A. (2001) *J. Mol. Biol.* **313,** 1093–1102
9. Csonka, L. N., and Epstein, W. (1996) in *Escherichia coli and Salmonella: Cellular and Molecular Biology* (Neidhart, F. C., ed) pp. 1210–1223, American Society for Microbiology, Washington, D. C.
10. Beale, S. L. (1996) in *Escherichia coli and Salmonella: Cellular and Molecular Biology* (Neidhart, F. C., ed) pp. 731–748, American Society for Microbiology, Washington, D. C.
11. Vanoni, M. A., and Curti, B. (1999) *Cell. Mol. Life Sci.* **55,** 617–638
12. Navarro, F., Martin-Figueroa, E., Candau, P., and Florencio, F. J. (2000) *Arch. Biochem. Biophys.* **379,** 267–276
13. Ravasio, S., Curti, B., and Vanoni, M. A. (2001) *Biochemistry* **40,** 5533–5541
14. Vanoni, M. A., Fischer, F., Ravasio, S., Verzotti, E., Edmondson, D. E., Hagen, W. R., Zanetti, G., and Curti, B. (1998) *Biochemistry* **37,** 1828–1838
15. Zalkin, H., and Smith, J. L. (1997) *Adv. Enzymol. Relat. Areas Mol. Biol.* **72,** 87–144
16. Binda, C., Bossi, R. T., Wakatsuki, S., Arzt, S., Coda, A., Curti, B., Vanoni, M. A., and Mattevi, A. (2000) *Structure* **8,** 1299–1308
17. Mozzarelli, A., and Rossi, G. L. (1996) *Annu. Rev. Biophys. Biomol. Struct.* **25,** 343–365
18. Leslie, A. G. (1999) *Acta Crystallogr. Sect. D Biol. Crystallogr.* **55,** 1696–1702
19. Computational Project Number 4 (1994) *Acta Crystallogr. Sect. D Biol. Crystallogr.* **50,** 760–767
20. Vagin, A., and Teplyakov, A. (1997) *J. Appl. Crystallogr.* **30,** 1022–1025
21. Cowtan, K. D., and Main, P. (1998) *Acta Crystallogr. Sect. D Biol. Crystallogr.* **54,** 487–593
22. Jones, T. A., Zou, J. Y., Cowan, S. W., and Kjeldgaard, M. (1991) *Acta Crystallogr. Sect. A* **47,** 110–119
23. Murshudov, G. N., Vagin, A. A., and Dodson, E. J. (1997) *Acta Crystallogr. Sect. D Biol. Crystallogr.* **53,** 240–255
24. Brünger, A. T. (1992) *Nature* **355,** 472–475
25. Lamzin, V. S., Wilson, K. S., Abrahams, J. P., and Leslie, A. G. W. (1993) *Acta Crystallogr. Sect. D Biol. Crystallogr.* **49,** 129–147
26. Lakowski, R. A., MacArthur, M. W., Moss, D. S., and Thornton, J. M. (1993) *J. Appl. Crystallogr.* **26,** 283–291
27. Kleywegt, G. J., and Jones, T. A. (1994) *Acta Crystallogr. Sect. D Biol. Crystallogr.* **50,** 178–185
28. Thompson, J. D., Higgins, D. G., and Gibson, T. J. (1994) *Nucleic Acids Res.* **22,** 4673–4680
29. Kraulis, P. J. (1991) *J. Appl. Crystallogr.* **24,** 946–950
30. Esnouf, R. M. (1997) *J. Mol. Graphics* **15,** 132–134
31. Merritt, E. A., and Bacon, D. J. (1997) *Methods Enzymol.* **277,** 505–524